

Preparing ground states of the XXZ model using the quantum annealing with inductively coupled superconducting flux qubits

Takashi Imoto

Research Center for Emerging Computing Technologies, National Institute of Advanced Industrial Science and Technology (AIST), 1-1-1 Umezono, Tsukuba, Ibaraki 305-8568, Japan.

Yuya Seki

Graduate School of Science and Technology, Keio University, Hiyoshi 3-14-1, Kohoku-ku, Yokohama 223-8522, Japan.

Yuichiro Matsuzaki

Research Center for Emerging Computing Technologies, National Institute of Advanced Industrial Science and Technology (AIST), 1-1-1 Umezono, Tsukuba, Ibaraki 305-8568, Japan.

E-mail: matsuzaki.yuichiro@aist.go.jp

Abstract. Preparing ground states of Hamiltonians is important in the condensed matter physics and the quantum chemistry. The interaction Hamiltonians typically contain not only diagonal but also off-diagonal elements. Although quantum annealing provides a way to prepare a ground state of a Hamiltonian, we can only use the Hamiltonian with Ising interaction by using currently available commercial quantum annealing devices. In this work, we propose a quantum annealing for the XXZ model, which contains both Ising interaction and energy-exchange interaction, by using inductively coupled superconducting flux qubits. The key idea is to use a recently proposed spin-lock quantum annealing where the qubits are driven by microwave fields. As long as the rotating wave approximation is valid, the inductive coupling between the superconducting flux qubits produces the desired Hamiltonian in the rotating frame, and we can use such an interaction for the quantum annealing while the microwave fields driving play a role of the transverse fields. To quantify the performance of our scheme, we implement numerical simulations, and show that we can prepare ground states of the two-dimensional Heisenberg model with a high fidelity.

1. Introduction

Quantum annealing (QA) is a method to solve the combinatorial optimization problem [1, 2, 3]. Combinatorial optimization problems can be mapped into problems of finding the ground state of an Ising model. In this case, the Ising model is the problem Hamiltonian. On the other

hand, we use the Hamiltonian of transverse fields to prepare an initial state, and this is called a drive Hamiltonian. In the QA, we prepare a ground state of the drive Hamiltonian, and then let the system evolve by a time dependent Hamiltonian to change from the drive Hamiltonian to the problem Hamiltonian in an adiabatic way. This provides a way to prepare a ground-state of the problem Hamiltonian as long as an adiabatic condition is satisfied.

There are many other applications of the quantum annealing in addition to combinatorial optimization problems. Firstly, quantum annealing can be used for machine learning. A way to learn binary machine learning models using the quantum annealing is reported [4, 5]. There are applications of the quantum annealing for clustering [6, 7]. A method of using the quantum annealing to perform calculations for the topological data analysis(TDA) was reported [8]. Quantum annealing has been applied as a sampling machine for restricted Boltzmann machines with deep layers [9, 10, 11, 12, 13]. Secondly, quantum annealing is known to be useful for quantum chemistry calculation. The Hamiltonian of molecules are written in the second quantized form. There are known methods to convert the second quantized form of the Hamiltonian into the spin Hamiltonian [14, 15, 16, 17, 18]. In quantum chemical calculations, it is important to obtain the energy of the molecules with high accuracy. When the energy is known to the so called chemical accuracy, a chemical reaction can be predicted [19]. In fact, calculations to determine the energy of molecules using quantum annealing have been reported [20, 21, 22, 23]. In addition, the method to measure similarity of the structures of molecules using the quantum annealing is proposed [24]. Finally, the quantum annealing can be applied to simulate condensed matter phenomena The \mathbb{Z}_2 spin liquid is emulated with the quantum annealing [25]. It has been reported that the KT(Kosterlitz–Thouless) phase transition was observed using a quantum annealing on the d-wave system [26]. Simulations of the Shastry-Sutherland Ising, a frustrated system, were performed using quantum annealing [27]. A phase transition of three dimensional transverse Ising model is detected using the quantum annealing machine [28]. It is worth mentioning that, in the previous demonstrations, the problem Hamiltonian was mapped into an Ising model, and this typically requires many ancillary qubits.

Superconducting flux qubits (FQs) are considered as promising systems for quantum information processing. The FQ is composed of a superconducting loop with Josephson junctions [29, 30, 31, 32]. It is possible to tune the energy gap of the FQ and the interaction between FQs [33, 34]. There are many attempts to improve the coherence time of the FQs [35, 36, 37]. Moreover, recently, a new design of the FQs called a capacitively shunted flux qubit with a long coherence time was proposed and demonstrated [38, 39, 40, 41]. The FQ can be used as a sensor to detect magnetic fields, electron spins, or defects [42, 43, 44, 45]. The FQs have advantages in a scalability, and actually it is possible to fabricate thousands of the FQs even in the current technology [46].

The company D-Wave Systems, Inc. realizes a quantum annealer with thousands of the FQs [47, 48]. The energy bias, energy gap, and the coupling between the FQs can be tuned by changing the applied magnetic flux. With currently available commercial quantum annealing devices, we can use only transverse field Ising model as the Hamiltonian where the flux qubits are inductively coupled. Recently, two flux qubits are coupled by using two

degree of freedoms, charge and flux [49]. In this case, not only Ising coupling but also energy-exchange interaction such as $\hat{\sigma}_x\hat{\sigma}_x$ (or $\hat{\sigma}_y\hat{\sigma}_y$) can be realized. However, this approach requires a complicated setup. It is preferable if we could construct the energy-exchange terms with less degree of freedom of the FQs.

In this paper, we propose a method to prepare a ground-state of the Hamiltonian that contains both Ising interaction and energy exchange interaction, which is the XXZ model, by using QA with the inductively coupled FQs. The key idea is to adopt a spin lock quantum annealing [50, 51, 52]. When we drive the FQs with the microwave fields, we can rewrite the Hamiltonian in a rotating frame with a frequency of the microwave fields. By using a rotating wave approximation, the inductive coupling between the FQs provides not only Ising interaction but also the energy exchange interaction. The driving with the microwave fields play a role of the driver Hamiltonian of the QA, and we can obtain a ground state of a Hamiltonian that contains both Ising and energy-exchange interaction by adiabatically turning off the driving fields. Such a preparation of the ground state allows us to calculate an arbitrary correlation function for the ground state of the XXZ model, which is useful in the condensed matter physics [53]. To quantify the performance of our scheme, we implement numerical simulations to prepare ground states of the two-dimensional Heisenberg model, and shows that we can achieve a high fidelity.

The paper is structured as follow. In Section 2, we review the conventional quantum annealing and spin lock quantum annealing. In Section 3, we show the method to create the energy exchange interaction by using the inductively coupled FQs for the QA. In Section 4, we perform numerical simulations to evaluate the performance of our method. In section 5, we summarize and discuss our results.

2. The previous work

In this section, let us review the conventional quantum annealing with DC fields and recently proposed quantum annealing with spin-lock technique.

2.1. Quantum annealing

In this subsection, we review the conventional quantum annealing. The annealing Hamiltonian is written as

$$H(t) = \frac{t}{T}H_P + \left(1 - \frac{t}{T}\right)H_D \quad (1)$$

where T is annealing time, H_P is the problem Hamiltonian, and H_D is the drive Hamiltonian. We define the drive Hamiltonian as follows

$$H_D = -B \sum_{j=1}^L \hat{\sigma}_j^{(x)} \quad (2)$$

where B denotes an amplitude of the DC transverse fields. After preparing a ground state of the drive Hamiltonian, we let the state evolve by the annealing Hamiltonian. If this dynamics

is adiabatic, the ground state of the drive Hamiltonian is changed into that of the problem Hamiltonian.

2.2. Spin lock quantum annealing

We review the spin-lock quantum annealing [50, 51, 52]. Unlike the conventional QA with the DC transverse fields, we use AC driving fields for the drive Hamiltonian when we adopt the spin-lock QA. Since the previous studies focus only on Ising interaction for the problem Hamiltonian, we consider such a case here. In the case of the spin lock quantum annealing, the annealing Hamiltonian is given by

$$H(\lambda) = B \sum_{j=1}^L \cos(\omega t) \hat{\sigma}_j^{(x)} + \sum_{j=1}^L \frac{\omega}{2} \hat{\sigma}_j^{(z)} + (1 - \lambda) H_P \quad (3)$$

where B denotes an amplitude of AC field, $\hat{\sigma}_j^{(k)}$ ($k = x, y, z$) denotes the Pauli operator acting on the j -th site of the spin chain, L is the site number, and H_P is the problem Hamiltonian. By moving to a rotating frame defined by U , the Hamiltonian is rewritten as

$$H' = U H U^\dagger - i U^\dagger \frac{dU}{dt} \quad (4)$$

Since we drive the qubits with the AC driving fields, we choose the operator U as follows

$$U = \exp\left(-i \frac{\omega}{2} t \sum_{j=1}^L \hat{\sigma}_j^{(z)}\right). \quad (5)$$

Here, we have

$$U^\dagger H_P U = H_P \quad (6)$$

and we can calculate as follows.

$$\begin{aligned} U \cos(\omega t) \hat{\sigma}_j^{(x)} U^\dagger &= \frac{1}{2} \left((e^{2i\omega t} + 1) \hat{\sigma}_j^{(+)} + (e^{-2i\omega t} + 1) \hat{\sigma}_j^{(-)} \right) \\ &\approx \frac{1}{2} \hat{\sigma}_j^{(x)}. \end{aligned} \quad (7)$$

where we use the rotating wave approximation. Throughout of this paper, we use the notation \approx to represent the rotating wave approximation. Using the relation

$$-i U^\dagger \frac{dU}{dt} = -\frac{\omega}{2} \sum_{j=1}^L \hat{\sigma}_j^{(z)}, \quad (8)$$

we obtain the annealing Hamiltonian in the rotating frame as follows.

$$H' \approx \sum_{j=1}^L \frac{\lambda}{2} \hat{\sigma}_j^{(x)} + (1 - \lambda) H_P \quad (9)$$

Therefore, we obtain the annealing Hamiltonian where the drive Hamiltonian is the transverse field in the rotating frame. It is worth mentioning that a violation of the the rotating wave approximation due to strong driving could cause an error in the preparation of the ground state [52].

3. Realization of the XXZ model using flux qubit

Here, we describe our scheme to prepare a ground state of the Hamiltonian with Ising interaction and energy-exchange interaction by using the spin-lock QA. Here, we consider a case that the flux qubits are inductively coupled. The Hamiltonian of the flux qubit [54, 55, 31] or capacitively shunted FQs [39] is given by

$$H = \frac{\epsilon}{2} \sum_{j=1}^L \hat{\sigma}_z^{(j)} + \frac{\Delta_G}{2} \sum_{j=1}^L \hat{\sigma}_x^{(j)} + \lambda \cos \omega t \sum_{j=1}^L \hat{\sigma}_y^{(j)} + g \sum_{j=1}^{L-1} \hat{\sigma}_z^{(j)} \hat{\sigma}_z^{(j+1)}. \quad (10)$$

where ϵ denotes an energy bias, Δ_G denotes an energy gap, g denotes a strength of the inductive interactions, and λ denotes a Rabi frequency. First, we use the single qubit operator $U_y \equiv e^{-i\theta \sum_{j=1}^L \hat{\sigma}_y^{(j)}}$ to rotate this Hamiltonian by θ in the y-direction.

$$\begin{aligned} H' &= U_y^{-1} H U_y \\ &= \left(\frac{\Delta_G}{2} \cos \theta - \frac{\epsilon}{2} \sin \theta \right) \sum_{j=1}^L \hat{\sigma}_x^{(j)} + \left(\frac{\epsilon}{2} \cos \theta + \frac{\Delta_G}{2} \sin \theta \right) \sum_{j=1}^L \hat{\sigma}_z^{(j)} + \lambda \cos \omega t \sum_{j=1}^L \hat{\sigma}_y^{(j)} \\ &\quad + g \sum_{j=1}^{L-1} \left(\cos^2 \theta \hat{\sigma}_z^{(j)} \hat{\sigma}_z^{(j+1)} + \sin^2 \theta \hat{\sigma}_x^{(j)} \hat{\sigma}_x^{(j+1)} - \cos \theta \sin \theta (\hat{\sigma}_z^{(j)} \hat{\sigma}_x^{(j+1)} + \hat{\sigma}_x^{(j)} \hat{\sigma}_z^{(j+1)}) \right) \end{aligned} \quad (11)$$

In order to remove the term of $\sum_{j=1}^L \hat{\sigma}_x^{(j)}$, we determine the θ as follows

$$\sin \theta = \frac{\Delta_G}{\sqrt{\epsilon^2 + \Delta_G^2}}, \quad (12)$$

$$\cos \theta = \frac{\epsilon}{\sqrt{\epsilon^2 + \Delta_G^2}}. \quad (13)$$

Next, the Hamiltonian in the interaction picture is given by

$$H'' = U^{-1} H' U - i U^{-1} \frac{dU}{dt} \quad (14)$$

where the single qubit operator U is defined as

$$U = e^{-\frac{i\omega t}{2} \sum_{j=1}^L \hat{\sigma}_z^{(j)}}. \quad (15)$$

Using the relation

$$-i U^{-1} \frac{dU}{dt} = -\frac{\omega}{2} \sum_{j=1}^L \hat{\sigma}_z^{(j)},$$

we obtain

$$\begin{aligned} H'' &= \lambda \cos \omega t U^{-1} \sum_{j=1}^L \hat{\sigma}_y^{(j)} U + \left(\frac{\epsilon}{2} \cos \theta + \frac{\Delta_G}{2} \sin \theta - \frac{\omega}{2} \right) U^{-1} \sum_{j=1}^L \hat{\sigma}_z^{(j)} U \\ &\quad + \sum_{j=1}^{L-1} g \left(\cos^2 \theta U^{-1} \hat{\sigma}_z^{(j)} \hat{\sigma}_z^{(j+1)} U + \sin^2 \theta U^{-1} \hat{\sigma}_x^{(j)} \hat{\sigma}_x^{(j+1)} U \right. \\ &\quad \left. - \cos \theta \sin \theta U^{-1} (\hat{\sigma}_z^{(j)} \hat{\sigma}_x^{(j+1)} + \hat{\sigma}_x^{(j)} \hat{\sigma}_z^{(j+1)}) U \right). \end{aligned} \quad (16)$$

We calculate each term of this Hamiltonian. The first term of this Hamiltonian is

$$\begin{aligned} \lambda \cos \omega t U^{-1} \hat{\sigma}_y^{(j)} U &= \frac{\lambda}{4i} \left(e^{2i\omega t} \hat{\sigma}_+^{(j)} + \hat{\sigma}_+^{(j)} - e^{-2i\omega t} \hat{\sigma}_-^{(j)} - \hat{\sigma}_-^{(j)} \right) \\ &\approx \frac{\lambda}{2} \hat{\sigma}_y^{(j)} \end{aligned} \quad (17)$$

by rotating wave approximation. We obtain the following

$$\begin{aligned} U^{-1} \hat{\sigma}_x^{(j)} \hat{\sigma}_x^{(j+1)} U &= e^{2i\omega t} \hat{\sigma}_+^{(j)} \hat{\sigma}_+^{(j+1)} + e^{-2i\omega t} \hat{\sigma}_-^{(j)} \hat{\sigma}_-^{(j+1)} + \hat{\sigma}_+^{(j)} \hat{\sigma}_-^{(j+1)} + \hat{\sigma}_-^{(j)} \hat{\sigma}_+^{(j+1)} \\ &\approx \hat{\sigma}_+^{(j)} \hat{\sigma}_-^{(j+1)} + \hat{\sigma}_-^{(j)} \hat{\sigma}_+^{(j+1)}. \end{aligned} \quad (18)$$

Also, we obtain

$$\begin{aligned} U^{-1} (\hat{\sigma}_z^{(j)} \hat{\sigma}_x^{(j+1)} + \hat{\sigma}_x^{(j)} \hat{\sigma}_z^{(j+1)}) U &= \hat{\sigma}_z^{(j)} (e^{i\omega t} \hat{\sigma}_+^{(j+1)} + e^{-i\omega t} \hat{\sigma}_-^{(j+1)}) + (e^{i\omega t} \hat{\sigma}_+^{(j)} + e^{-i\omega t} \hat{\sigma}_-^{(j)}) \hat{\sigma}_z^{(j+1)} \\ &\approx 0. \end{aligned} \quad (19)$$

Finally, the other terms are unaffected by the operator U . Therefore, substituting the Eq. (17), (18) and, (19) into the Eq. (16), we obtain the

$$\begin{aligned} H'' &\approx \frac{\lambda}{2} \sum_{j=1}^L \hat{\sigma}_y^{(j)} + \Delta\omega \sum_{j=1}^L \hat{\sigma}_z^{(j)} \\ &\quad + g \sum_{j=1}^{L-1} \left(\frac{\epsilon^2}{\epsilon^2 + \Delta_G^2} \hat{\sigma}_z^{(j)} \hat{\sigma}_z^{(j+1)} + \frac{\Delta_G^2}{\epsilon^2 + \Delta_G^2} (\hat{\sigma}_+^{(j)} \hat{\sigma}_-^{(j+1)} + \hat{\sigma}_-^{(j)} \hat{\sigma}_+^{(j+1)}) \right) \end{aligned} \quad (20)$$

where the detuning is defined as $\delta\omega = \left(\frac{\epsilon^2}{2\sqrt{\epsilon^2 + \Delta_G^2}} + \frac{\Delta_G^2}{2\sqrt{\epsilon^2 + \Delta_G^2}} - \frac{\omega}{2} \right)$. By rotating the Hamiltonian by $\pi/2$ along the z axis, we obtain the Hamiltonian with the transverse field parallel to the x axis. This means that, by changing λ and g , we can perform the QA where the driver Hamiltonian is the transverse field and the problem Hamiltonian is the XXZ model. Throughout of our paper, we take $\lambda(t) = \lambda(0)\frac{t}{T}$ and $g(t) = g(0)(1 - \frac{t}{T})$. Moreover, since we have not only the transverse field parallel to the x axis but also the longitudinal field, we could construct a driver Hamiltonian with twisted fields, which is shown to be useful to obtain a ground state with the QA [56, 57]. However, in our paper, we focus on the resonant case with $\delta\omega = 0$.

4. Application and numerical simulation

In this section, in order to evaluate the performance of our scheme, we perform numerical simulations. For the problem Hamiltonians, we consider an example of a two dimensional anisotropic Heisenberg model in condensed matter physics.

The problem Hamiltonian is given by

$$H_P = J \sum_{\langle j,k \rangle} \left(\sigma_j^{(x)} \sigma_k^{(x)} + \sigma_j^{(y)} \sigma_k^{(y)} + \Delta \sigma_j^{(z)} \sigma_k^{(z)} \right). \quad (21)$$

where Δ denotes the anisotropic parameter, and J denotes the coupling constant. This is called the ferro magnetic model when $J < 0$, and anti-ferro magnetic model when $J > 0$.

To realize this problem Hamiltonian in the spin lock we set $J = g \frac{\epsilon^2}{\epsilon^2 + \Delta_G^2}$ and $\Delta = \frac{\Delta_G^2}{\epsilon^2}$. We consider a square lattice of size 2×3 , as shown in Figure.1. About the coupling constants J

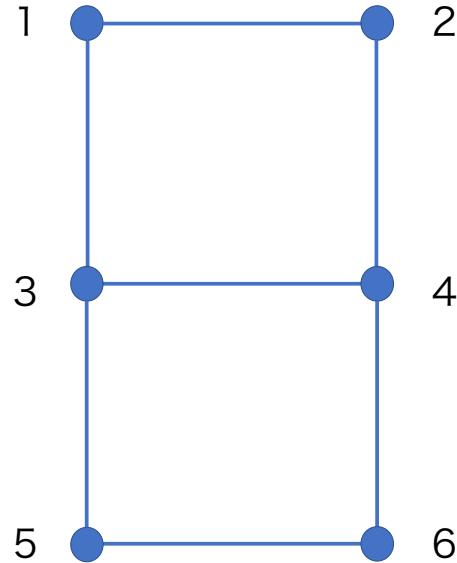


Figure 1: Schematic of our model.

and anisotropic parameters Δ , we consider the following four cases.

$$(J, \Delta) = (1, 1.7), (1, 0.7), (-1, 1.7), (-1, 0.7). \quad (22)$$

where the unit of the value of J is GHz, as shown in Figure.2.

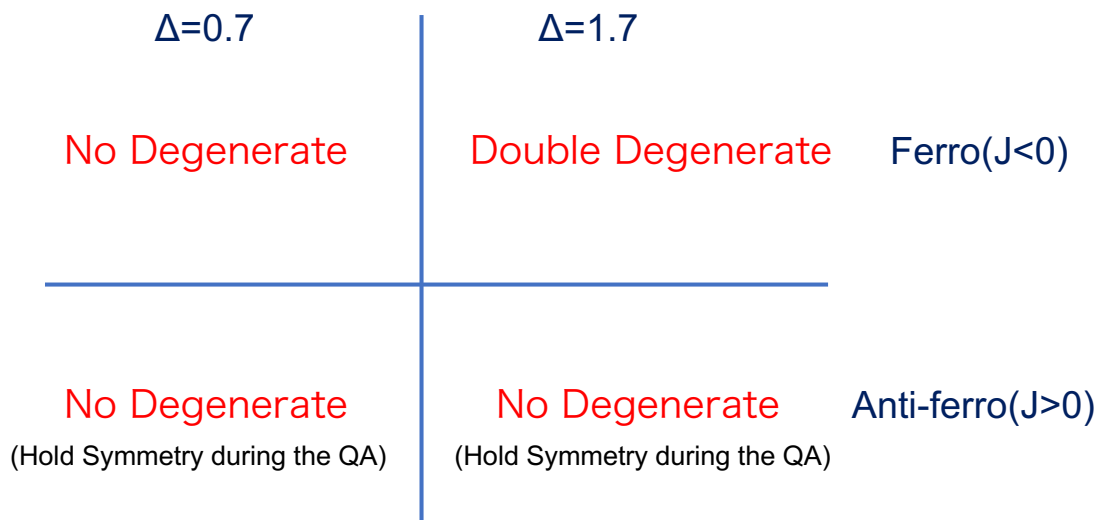


Figure 2: A conceptual diagram of the anisotropic Heisenberg model.

The ground state was found to be doubly degenerate in the case of ferro-magnetic coupling ($J = -1$) and $\Delta = 1.7$. On the other hand, the ground state is not degenerate

in the other cases. Throughout of our manuscript, when we plot a fidelity F , we calculate $F = \sum_{n=1}^m \langle g_n | \rho(t) | g_n \rangle$ where m denotes the degeneracy, $\{|g_n\rangle\}_{n=1}^m$ denotes the ground state, and $\rho(t)$ denotes a quantum state after the QA.

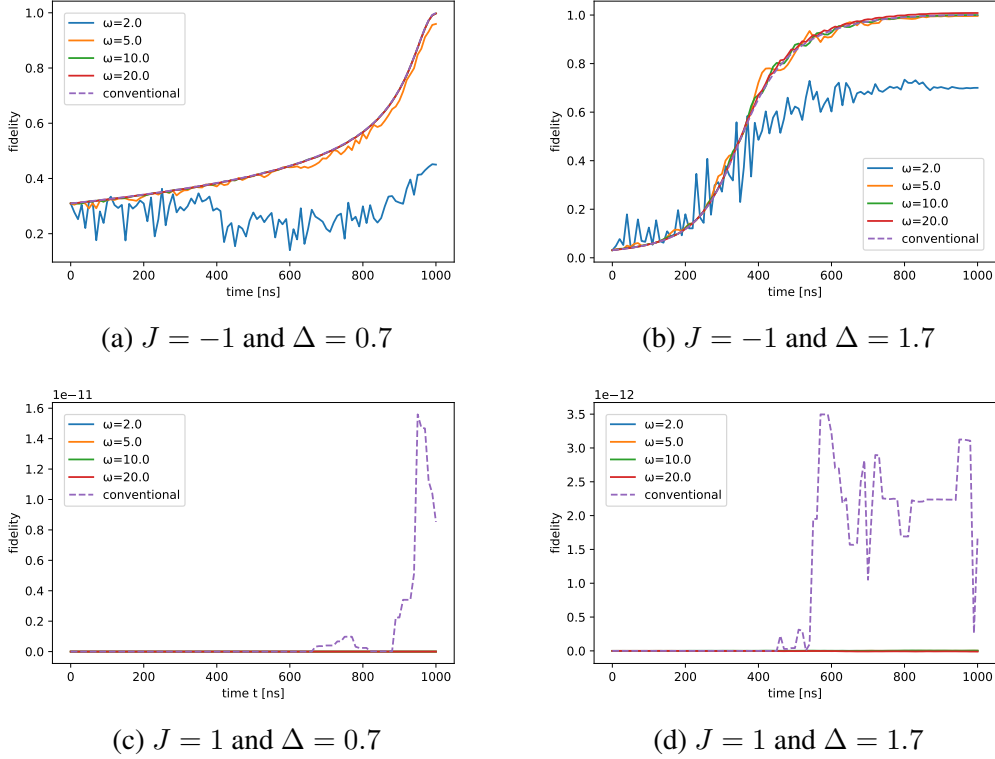


Figure 3: Fidelity between the ground state of the two-dimensional anisotropic Heisenberg model and the state during QA against time. The parameters for the simulation are chosen as $T = 1000$ ns, $\lambda = 1$ and, $\omega = 2.0, 5.0, 10.0, 20.0$ GHz. We adopt the uniform microwave driving (DC transverse fields) as the drive Hamiltonian for our (conventional) scheme.

We plot the fidelity against time for each frequency ω with numerical simulations in the Figure 3. For these simulations, the annealing time T is set to be 1000 [ns], the driving strength λ is set to be 1 GHz, and the frequencies ω are set to be 2.0, 5.0, 10.0, 20.0 GHz. For the ferro magnetic case, as we increase the frequency ω , the fidelity increases. This is consistent with the fact that the rotating wave approximation becomes more accurate as the qubit frequency increases. Thus, after the preparation of the ground state with a high fidelity, we can measure an arbitrary correlation function for the ground state of the Hamiltonian, which is useful in the condensed matter physics.

In the case of anti-ferro magnetic ($J = 1$ GHz), for $\Delta = 0.7$ and $\Delta = 1.7$, the fidelities are zero up to numerical errors. Our considerations suggest that there is a symmetry during QA for these parameters. In general, when there is a symmetry, the total Hamiltonian commutes with some observables. In this case, the Hamiltonian can be block diagonalized into sectors by applying a suitable unitary operator. As long as the initial state belongs to a different sector from that to which the target ground state belongs, we cannot prepare a ground

state even after the QA by keeping the adiabatic condition because a level crossing occurs. Actually, in our case, we confirm that an operator $U_{swap}^{(1,2)}U_{swap}^{(3,4)}U_{swap}^{(5,6)}$ commutes with both the transverse field and the ferromagnetic XXZ model Hamiltonian where $U_{swap}^{(j,k)}$ denotes a swap gate between the j -th qubit and the k -th qubit. We calculate the sector of $U_{swap}^{(1,2)}U_{swap}^{(3,4)}U_{swap}^{(5,6)}$ for the ground states of the transvers field and the ferromagnetic XXZ model, and we obtain $\langle E_0^{(TF)} | U_{swap}^{(1,2)}U_{swap}^{(3,4)}U_{swap}^{(5,6)} | E_0^{(TF)} \rangle = 1$ and $\langle E_0^{(XXZ)} | U_{swap}^{(1,2)}U_{swap}^{(3,4)}U_{swap}^{(5,6)} | E_0^{(XXZ)} \rangle = -1$ where $|E_0^{(TF)}\rangle$ denotes the ground state of the transvers field and $|E_0^{(XXZ)}\rangle$ denotes the ground state of the XXZ model. Therefore, we can confirm that $|E_0^{(TF)}\rangle$ and $|E_0^{(XXZ)}\rangle$ belong to different sectors, and this is the reason why the QA fails in our numerical simulations.

J_1	-0.9052919617126958
J_2	0.2500243810835503
J_3	-1.931378367720707
J_4	-0.007622719480759765
J_5	-1.259154537693434
J_6	-1.261510983981174

Table 1: Coefficients of random transverse field $\{J_j\}_{j=1}^6$ used in Fig. 4. The unit of these values is GHz, as described in the main text.

In such a case, we apply not homogeneous but randomized microwave driving (DC transverse fields) to break the symmetry for our (conventional) scheme. Moreover, we plot the fidelities against time when we apply the randomized driving Hamiltonian in the Figure. 4. This demonstrates that we can prepare a ground state with a high fidelity by using the randomized fields during QA without level crossing. Also, our results show that a proper choice of the driver Hamiltonian to break a symmetry of the Hamiltonian is important in QA, which has been overlooked in previous works.

5. Conclusion

In conclusion, we propose the way to prepare a ground state of the XXY model with the QA by using inductively coupled superconducting flux qubits. The key idea is to use a recently proposed spin-lock quantum annealing. We drive the flux qubits by the microwave driving, and we can construct the Hamiltonian of QA for the XXY model in the rotating frame. By choosing the problem Hamiltonian as the anisotropic Heisenberg model, we can prepare a ground state of the anisotropic Heisenberg model with our scheme unless there is a level crossing. Importantly, when there is a symmetry during QA, the Hamiltonian can be block diagonalized into sectors. As long as the initial state belongs to a different sector from that to which the target ground state belongs, we cannot prepare the ground state with QA because of the level crossing. In this case, we show that, by adding randomized fields to break the symmetry, we can avoid the problem of the level crossing. Our numerical simulation shows that our spin-lock QA actually provides a practical way to prepare a ground state. Our scheme

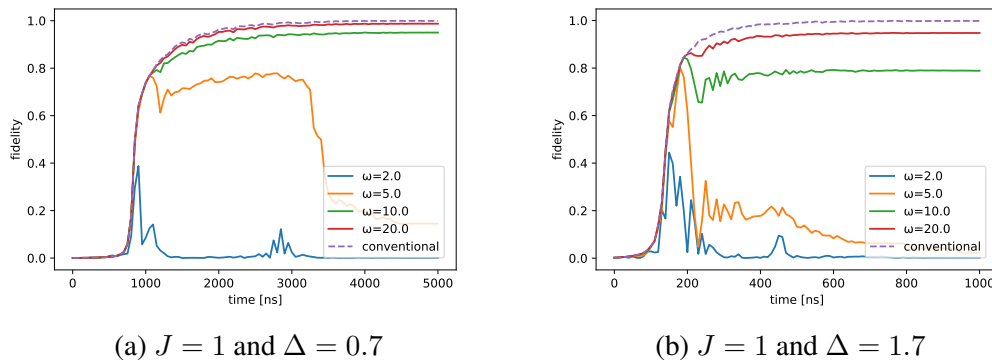


Figure 4: We plot the fidelity between the ground state of the two-dimensional anisotropic Heisenberg model and the state during QA against time. The parameters for the simulation are chosen as, $T = 1000$ ns, and $\omega = 2.0, 5.0, 10.0, 20.0$ GHz. In order to break the symmetry, we adopt the random microwave driving (DC transverse field) as the drive Hamiltonian for our (conventional) scheme.

is useful to know the correlation function of the relevant Hamiltonians in the condensed matter physics.

Note added.—While preparing our manuscript, we became aware of a related work that also proposes an adiabatic scheme to prepare a ground state of a Hamiltonian (that contains non-diagonal terms) by applying additional fields to break the symmetry [58].

Acknowledgments

We thank S. Kawabata and A. Yoshinaga for a useful advice. This work was supported by MEXT’s Leading Initiative for Excellent Young Researchers and JST PRESTO (Grant No. JPMJPR1919), Japan. This paper is partly based on the results obtained from a project, JPNP16007, commissioned by the New Energy and Industrial Technology Development Organization (NEDO), Japan.

References

- [1] Tadashi Kadowaki and Hidetoshi Nishimori. Quantum annealing in the transverse ising model. *Physical Review E*, 58(5):5355, 1998.
- [2] Edward Farhi, Jeffrey Goldstone, Sam Gutmann, and Michael Sipser. Quantum computation by adiabatic evolution. *arXiv preprint quant-ph/0001106*, 2000.
- [3] Edward Farhi, Jeffrey Goldstone, Sam Gutmann, Joshua Lapan, Andrew Lundgren, and Daniel Preda. A quantum adiabatic evolution algorithm applied to random instances of an np-complete problem. *Science*, 292(5516):472–475, 2001.
- [4] Prasanna Date and Thomas Potok. Adiabatic quantum linear regression. 2020.
- [5] Michele Sasdelli and Tat-Jun Chin. Quantum annealing formulation for binary neural networks. *arXiv preprint arXiv:2107.02751*, 2021.
- [6] Kenichi Kurihara, Shu Tanaka, and Seiji Miyashita. Quantum annealing for clustering. In *25th Conference on Uncertainty in Artificial Intelligence, UAI 2009*, 2009.

- [7] Vaibhaw Kumar, Gideon Bass, Casey Tomlin, and Joseph Dulny. Quantum annealing for combinatorial clustering. *Quantum Information Processing*, 17(2):1–14, 2018.
- [8] Jesse J Berwald, Joel M Gottlieb, and Elizabeth Munch. Computing wasserstein distance for persistence diagrams on a quantum computer. *arXiv preprint arXiv:1809.06433*, 2018.
- [9] Steven H Adachi and Maxwell P Henderson. Application of quantum annealing to training of deep neural networks. *arXiv preprint arXiv:1510.06356*, 2015.
- [10] Max Wilson, Thomas Vandal, Tad Hogg, and Eleanor G Rieffel. Quantum-assisted associative adversarial network: Applying quantum annealing in deep learning. *Quantum Machine Intelligence*, 3(1):1–14, 2021.
- [11] Richard Y Li, Tameem Albash, and Daniel A Lidar. Limitations of error corrected quantum annealing in improving the performance of boltzmann machines. *Quantum Science and Technology*, 5(4):045010, 2020.
- [12] Hartmut Neven, Vasil S Denchev, Geordie Rose, and William G Macready. Training a binary classifier with the quantum adiabatic algorithm. *arXiv preprint arXiv:0811.0416*, 2008.
- [13] Walter Winci, Lorenzo Buffoni, Hossein Sadeghi, Amir Khoshaman, Evgeny Andriyash, and Mohammad H Amin. A path towards quantum advantage in training deep generative models with quantum annealers. *Machine Learning: Science and Technology*, 1(4):045028, 2020.
- [14] Sergey B Bravyi and Alexei Yu Kitaev. Fermionic quantum computation. *Annals of Physics*, 298(1):210–226, 2002.
- [15] Frank Verstraete and J Ignacio Cirac. Mapping local hamiltonians of fermions to local hamiltonians of spins. *Journal of Statistical Mechanics: Theory and Experiment*, 2005(09):P09012, 2005.
- [16] Jacob T Seeley, Martin J Richard, and Peter J Love. The bravyi-kitaev transformation for quantum computation of electronic structure. *The Journal of chemical physics*, 137(22):224109, 2012.
- [17] Andrew Tranter, Sarah Sofia, Jake Seeley, Michael Kaicher, Jarrod McClean, Ryan Babbush, Peter V Coveney, Florian Mintert, Frank Wilhelm, and Peter J Love. The bravyi-kitaev transformation: Properties and applications. *International Journal of Quantum Chemistry*, 115(19):1431–1441, 2015.
- [18] Rongxin Xia, Teng Bian, and Sabre Kais. Electronic structure calculations and the ising hamiltonian. *The Journal of Physical Chemistry B*, 122(13):3384–3395, 2017.
- [19] Henry Eyring. The activated complex in chemical reactions. *The Journal of Chemical Physics*, 3(2):107–115, 1935.
- [20] Justin Copenhaver, Adam Wasserman, and Birgit Wehefritz-Kaufmann. Using quantum annealers to calculate ground state properties of molecules. *The Journal of Chemical Physics*, 154(3):034105, 2021.
- [21] Guglielmo Mazzola, Vadim N Smelyanskiy, and Matthias Troyer. Quantum monte carlo tunneling from quantum chemistry to quantum annealing. *Physical Review B*, 96(13):134305, 2017.
- [22] Scott N Genin, Ilya G Ryabinkin, and Artur F Izmaylov. Quantum chemistry on quantum annealers. *arXiv preprint arXiv:1901.04715*, 2019.
- [23] Michael Streif, Florian Neukart, and Martin Leib. Solving quantum chemistry problems with a d-wave quantum annealer. In *International Workshop on Quantum Technology and Optimization Problems*, pages 111–122. Springer, 2019.
- [24] Maritza Hernandez and Maliheh Aramon. Enhancing quantum annealing performance for the molecular similarity problem. *Quantum Information Processing*, 16(5):133, 2017.
- [25] Shiyu Zhou, Dmitry Green, Edward D Dahl, and Claudio Chamon. Experimental realization of classical z_2 spin liquids in a programmable quantum device. *Physical Review B*, 104(8):L081107, 2021.
- [26] Andrew D King, Juan Carrasquilla, Jack Raymond, Isil Ozfidan, Evgeny Andriyash, Andrew Berkley, Mauricio Reis, Trevor Lanting, Richard Harris, Fabio Altomare, et al. Observation of topological phenomena in a programmable lattice of 1,800 qubits. *Nature*, 560(7719):456–460, 2018.
- [27] Paul Kairys, Andrew D King, Isil Ozfidan, Kelly Boothby, Jack Raymond, Arnab Banerjee, and Travis S Humble. Simulating the shastry-sutherland ising model using quantum annealing. *PRX Quantum*, 1(2):020320, 2020.
- [28] R Harris, Y Sato, AJ Berkley, M Reis, F Altomare, MH Amin, K Boothby, P Bunyk, C Deng, C Enderud, et al. Phase transitions in a programmable quantum spin glass simulator. *Science*, 361(6398):162–165,

- 2018.
- [29] JE Mooij, TP Orlando, L Levitov, Lin Tian, Caspar H Van der Wal, and Seth Lloyd. Josephson persistent-current qubit. *Science*, 285(5430):1036–1039, 1999.
 - [30] TP Orlando, JE Mooij, Lin Tian, Caspar H Van Der Wal, LS Levitov, Seth Lloyd, and JJ Mazo. Superconducting persistent-current qubit. *Physical Review B*, 60(22):15398, 1999.
 - [31] John Clarke and Frank K Wilhelm. Superconducting quantum bits. *Nature*, 453(7198):1031–1042, 2008.
 - [32] Yuriy Makhlin, Gerd Schön, and Alexander Shnirman. Quantum-state engineering with josephson-junction devices. *Reviews of modern physics*, 73(2):357, 2001.
 - [33] FG Paauw, A Fedorov, CJP M Harmans, and JE Mooij. Tuning the gap of a superconducting flux qubit. *Physical review letters*, 102(9):090501, 2009.
 - [34] AO Niskanen, K Harrabi, F Yoshihara, Y Nakamura, S Lloyd, and Jaw Shen Tsai. Quantum coherent tunable coupling of superconducting qubits. *Science*, 316(5825):723–726, 2007.
 - [35] Guido Burkard, David P DiVincenzo, P Bertet, I Chiorescu, and JE Mooij. Asymmetry and decoherence in a double-layer persistent-current qubit. *Physical Review B*, 71(13):134504, 2005.
 - [36] F Yoshihara, K Harrabi, AO Niskanen, Y Nakamura, and Jaw Shen Tsai. Decoherence of flux qubits due to $1/f$ flux noise. *Physical review letters*, 97(16):167001, 2006.
 - [37] Jonas Bylander, Simon Gustavsson, Fei Yan, Fumiki Yoshihara, Khalil Harrabi, George Fitch, David G Cory, Yasunobu Nakamura, Jaw-Shen Tsai, and William D Oliver. Noise spectroscopy through dynamical decoupling with a superconducting flux qubit. *Nature Physics*, 7(7):565–570, 2011.
 - [38] JQ You, Xuedong Hu, S Ashhab, and Franco Nori. Low-decoherence flux qubit. *Physical Review B*, 75(14):140515, 2007.
 - [39] Fei Yan, Simon Gustavsson, Archana Kamal, Jeffrey Birenbaum, Adam P Sears, David Hover, Ted J Gudmundsen, Danna Rosenberg, Gabriel Samach, Steven Weber, et al. The flux qubit revisited to enhance coherence and reproducibility. *Nature communications*, 7(1):1–9, 2016.
 - [40] Antonio D Córcoles, Jerry M Chow, Jay M Gambetta, Chad Rigetti, James R Rozen, George A Keefe, Mary Beth Rothwell, Mark B Ketchen, and Matthias Steffen. Protecting superconducting qubits from radiation. *Applied Physics Letters*, 99(18):181906, 2011.
 - [41] Matthias Steffen, Shwetank Kumar, David P DiVincenzo, JR Rozen, George A Keefe, Mary Beth Rothwell, and Mark B Ketchen. High-coherence hybrid superconducting qubit. *Physical review letters*, 105(10):100502, 2010.
 - [42] Mustafa Bal, Chunqing Deng, Jean-Luc Orgiazzi, FR Ong, and Adrian Lupascu. Ultrasensitive magnetic field detection using a single artificial atom. *Nature communications*, 3(1):1–8, 2012.
 - [43] Hiraku Toida, Yuichiro Matsuzaki, Kosuke Kakuyanagi, Xiaobo Zhu, William J Munro, Hiroshi Yamaguchi, and Shiro Saito. Electron paramagnetic resonance spectroscopy using a single artificial atom. *Communications Physics*, 2(1):1–7, 2019.
 - [44] Ranga P Budoyo, Kosuke Kakuyanagi, Hiraku Toida, Yuichiro Matsuzaki, and Shiro Saito. Electron spin resonance with up to 20 spin sensitivity measured using a superconducting flux qubit. *Applied Physics Letters*, 116(19):194001, 2020.
 - [45] Leonid V Abdurakhimov, Imran Mahboob, Hiraku Toida, Kosuke Kakuyanagi, Yuichiro Matsuzaki, and Shiro Saito. Driven-state relaxation of a coupled qubit-defect system in spin-locking measurements. *Physical Review B*, 102(10):100502, 2020.
 - [46] Kosuke Kakuyanagi, Yuichiro Matsuzaki, Corentin Déprez, Hiraku Toida, Kouichi Semba, Hiroshi Yamaguchi, William J Munro, and Shiro Saito. Observation of collective coupling between an engineered ensemble of macroscopic artificial atoms and a superconducting resonator. *Physical review letters*, 117(21):210503, 2016.
 - [47] Mark W Johnson, Mohammad HS Amin, Suzanne Gildert, Trevor Lanting, Firas Hamze, Neil Dickson, Richard Harris, Andrew J Berkley, Jan Johansson, Paul Bunyk, et al. Quantum annealing with manufactured spins. *Nature*, 473(7346):194–198, 2011.
 - [48] Sergio Boixo, Troels F Rønnow, Sergei V Isakov, Zhihui Wang, David Wecker, Daniel A Lidar, John M Martinis, and Matthias Troyer. Evidence for quantum annealing with more than one hundred qubits. *Nature physics*, 10(3):218–224, 2014.

- [49] Isil Ozfidan, Chunqing Deng, AY Smirnov, T Lanting, R Harris, L Swenson, J Whittaker, F Altomare, M Babcock, C Baron, et al. Demonstration of a nonstoquastic hamiltonian in coupled superconducting flux qubits. *Physical Review Applied*, 13(3):034037, 2020.
- [50] Hongwei Chen, Xi Kong, Bo Chong, Gan Qin, Xianyi Zhou, Xinhua Peng, and Jiangfeng Du. Experimental demonstration of a quantum annealing algorithm for the traveling salesman problem in a nuclear-magnetic-resonance quantum simulator. *Physical Review A*, 83(3):032314, 2011.
- [51] Mikio Nakahara. *Lectures on quantum computing, thermodynamics and statistical physics*, volume 8. World Scientific, 2013.
- [52] Yuichiro Matsuzaki, Hideaki Hakoshima, Yuya Seki, and Shiro Kawabata. Quantum annealing with capacitive-shunted flux qubits. *Japanese Journal of Applied Physics*, 59(SG):SGGI06, 2020.
- [53] Subir Sachdev. *Quantum phase transitions*. Cambridge university press, 2011.
- [54] Jonathan R Friedman, Vijay Patel, Wei Chen, SK Tolpygo, and James E Lukens. Quantum superposition of distinct macroscopic states. *nature*, 406(6791):43–46, 2000.
- [55] Caspar H Van Der Wal, ACJ Ter Haar, FK Wilhelm, RN Schouten, CJPM Harmans, TP Orlando, Seth Lloyd, and JE Mooij. Quantum superposition of macroscopic persistent-current states. *Science*, 290(5492):773–777, 2000.
- [56] Takashi Imoto, Yuya Seki, Yuichiro Matsuzaki, and Shiro Kawabata. Quantum annealing with twisted fields. *arXiv preprint arXiv:2111.15283*, 2021.
- [57] Tadashi Kadowaki and Hidetoshi Nishimori. Greedy parameter optimization for diabatic quantum annealing. *arXiv preprint arXiv:2111.13287*, 2021.
- [58] Akhil Francis, Ephrata Zelleke, Ziyue Zhang, Alexander F Kemper, and JK Freericks. Determining ground-state phase diagrams on quantum computers via a generalized application of adiabatic state preparation. *arXiv preprint arXiv:2112.04625*, 2021.